

Supporting Information

Construction of uniform buried pn junctions on pyramid Si photocathodes using a facile and safe spin-on method for photoelectrochemical water splitting

He Li^{ab}, Bin Liu^{ab}, Shijia Feng^{ab}, Huimin Li^{ab}, Tuo Wang^{*ab}, Jinlong Gong^{ab}

^aKey Laboratory for Green Chemical Technology of Ministry of Education, School of Chemical Engineering and Technology, Tianjin University, Tianjin 300072, China

^b Collaborative Innovation Center of Chemical Science and Engineering (Tianjin), Tianjin University, Tianjin 300072, China

Corresponding Authors

*E-mail: wangtuo@tju.edu.cn; Fax: +86 22 87401818

Materials

Ammonium dihydrogen phosphate ($\text{NH}_4\text{H}_2\text{PO}_4$, $\geq 99.99\%$) was purchased from Shanghai Aladdin Biochemical Technology. Ammonium hydroxide (NH_4OH , 25.0%), potassium hydroxide (KOH , $\geq 85.0\%$), hydrofluoric acid (HF , $\geq 40.0\%$) and chloroplatinic acid (H_2PtCl_6 , $\geq 99.0\%$) were purchased from Tianjin Kemiou Chemical Reagent Co., Ltd. Perchloric acid was supplied by Tianjin Xinqiao Chemical Trading Co., Ltd. Hydrogen peroxide (H_2O_2 , $\geq 30.0\%$) was purchased from Tianjin Jiangtian Chemical Technology Co., Ltd. Hydrochloric acid (HCl , 36%-38%), concentrated sulfuric acid (H_2SO_4 , 95%-98%) and isopropyl alcohol ($\text{C}_3\text{H}_8\text{O}$, $\geq 99.0\%$) were purchased by Tianjin Yuanli Chemical Co., Ltd. Titanium (IV)i-propoxide (TTIP, 99.999%) was supplied by Suzhou Fornano Electronics Technology Co., Ltd. High purity water ($18.25 \text{ M}\Omega \cdot \text{cm}$) supplied by a UP Water Purification System was used in the whole experimental processes. Single-crystalline p-Si (100) wafers (one-side polished) with a starting thickness of $500 \mu\text{m}$, diameter of 4 inches and resistivity of $1\text{-}10 \Omega \text{ cm}$ were obtained from Hefei Kejing Material Technology Co., Ltd. The SOD polymer solution used here is dopant P 509 which was commercially available from Filmtronics Co. (USA). The proton exchange membrane used in our work to separate two electrolytes is Nafion-115 from DuPont.

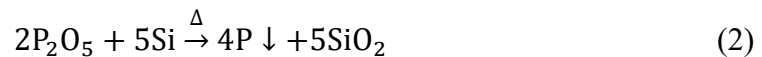
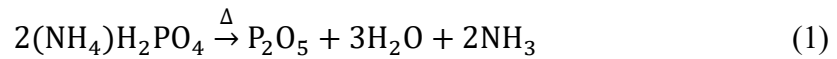
Wet etching

The pyramidal surface textured (pyramid) silicon substrate was produced by a chemical etching method. First of all, the Si wafer was boiled and cleaned with a full Radio Corporation of America (RCA) cleaning method (RCA1: $\text{NH}_4\text{OH}:\text{H}_2\text{O}_2:\text{H}_2\text{O} = 1:1:5$ for 10 minutes at 70°C ; RCA2: $\text{HCl}:\text{H}_2\text{O}_2:\text{H}_2\text{O} = 1:1:6$ for 10 minutes at 70°C). The purpose of the RCA cleaning is to remove the attached particles, organic matters and metal ions from the surface of the wafer. The randomly distributed pyramid Si was

then fabricated through anisotropic etching in a mixture solution of potassium hydroxide (KOH) (6 wt%) and isopropanol (3 vol%) at 80 °C for 25 min. The magnetic stir bar was maintained in constant rotation during the etching process to maintain the uniformity of temperature and concentration. After that, the sample was removed and cleaned again as in the first step. Finally, the wafer was rinsed with high purity water and blow-dried with nitrogen.

Fabrication of pn⁺Si

In this work, ADP aqueous solution as the phosphorous dopant source was prepared by dissolving ADP in high purity water, concentration is 5 wt%. The ADP aqueous solution was spun onto the front side of Si wafer at a speed of 4000 rpm, followed by baking at 100 °C for 10 minutes. Subsequently, the Si wafer spin-coated with ADP aqueous solution was annealed in an open quartz tube furnace at 950 °C for 1 hour. The formulas are as follows:



After the annealing process, the residual phosphosilicate glass was removed entirely with 5 vol% HF solution at room temperature for 3 minutes. The process of using SOD polymer solution as phosphorous dopant source was same as described above while the spin speed was 3000 rpm according to its instruction manual. Aluminum back contact was produced by depositing Al film onto the back side of Si wafers and then annealing in N₂ atmosphere at 800 °C for 10 minutes. Al film was deposited by using direct current (DC) magnetron sputtering with a working power of 40 W for 20 minutes.

Atomic layer deposition of TiO₂ thin film

TiO₂ thin film was deposited onto pyramid p⁺Si at 250 °C in a home-made atomic layer deposition (ALD) system using TTIP and H₂O as precursors. The precursors were held at 70 °C and 25 °C respectively. One ALD cycle consists of TTIP dose for 3 s, N₂ purge for 8 s, water dose for 0.2 s and N₂ (Air Liquid) purge for 8 s. 670 cycles of TiO₂ were deposited onto pyramid p⁺Si. The ALD TiO₂ growth on p-Si (100) substrate was measured by the M-2000 spectroscopic ellipsometer (J.A. Woollam).

Cocatalyst deposition

In order to enhance the kinetics for water reduction reaction, Pt nanoparticles were deposited by photo-electrodeposition until 50 mC passed through the Si electrode. The photo-electrodeposition is performed at an applied potential of 0 V vs. Ag/AgCl (3 M KCl) on the work electrode under simulated AM 1.5G illumination. The electrolyte was 1 mM aqueous solution of H₂PtCl₆ (using H₂SO₄ adjusts to pH < 1). The Si back side was attached with a cooper belt using conductive silver paint and the entire electrode was encapsulated with epoxy on slide glass before platinization. The active area without covered by epoxy was determined by a digital camera and ImageJ software.

Photoanode construction

The BiVO₄ film was synthesized on FTO substrates by metalorganic decomposition (MOD) method using dimethyl sulfoxide (DMSO) as the solvent to dissolve both Bi and V precursors simultaneously. 0.2425 g bismuth nitrate pentahydrate Bi(NO₃)₃·5H₂O and 0.1325 g vanadyl acetylacetonate VO(acac)₂ are mixed in 500 μL DMSO and sonicated for 30 min at room temperature. FTO substrate is preheated on the hotplate at 60 °C, and the film is deposited onto FTO by spin coating at 1000 rpm for 20 s followed by 3000 rpm for 40 s. Then the samples were calcined in a tube furnace at 500 °C for 2 h in the air. The obtained samples were soaked in 1 M KOH for 5 min to remove the surface VO_x species. Finally, BiVO₄ photoanode was

immersed in 1 M KBi buffer solution containing 0.2 M Na₂SO₃ with simulated AM 1.5 G illumination for 10 min, during which photo-induced etching of the surface region of amorphous BiVO₄ is removed to obtain enhanced surface oxygen vacancies.

CoO_x nanoparticles were synthesized by a typical hydrothermal method. In a typical procedure, 0.4 mL ammonium solution (NH₃·H₂O, 25 wt%) was added into 25 mL 1 mM cobalt acetate ethanol solution, followed by stirring for 15 min. Then the solution was transferred to a 50 mL Teflon-lined stainless steel autoclave. The hydrothermal synthesis was conducted at 120 °C for 1 h. The obtained products were centrifuged, washed with deionized water and ethanol for three times, respectively. Lastly, the obtained samples were dried in 80 °C for 12 h in a drying oven. The BiVO₄/CoO_x photoanode was fabricated by a drop-casting technique. Firstly, 20 mg of CoO_x nanoparticles were dispersed in 100 mL absolute ethanol and sonicated for 30 min to form a uniform nanoparticle “ink”. Then 100 μL “ink” was drop-casted onto a 1 cm² BiVO₄ electrode. The composites were fully dried at 80 °C for 30 min and then annealed at 450 °C for 2 h¹.

Structural and optical characterization

The morphology and microstructure of the samples were characterized using a field emission scanning electron microscope (FE-SEM, Hitachi S-4800, 5 kV) with an energy-dispersive X-ray (EDX) detector. The light absorption of as-prepared samples was obtained using a Shimadzu UV-2550 spectrophotometer equipped with an integrating sphere using BaSO₄ as the reflectance standard. Steady-state photoluminescence (PL) spectroscopy was performed on Hitachi F-4600 fluorescence spectrophotometer with 238 nm as the excitation wavelength. X-ray photoemission spectroscopy (XPS) analysis of the samples was carried out on a Physical Electronics

PHI 1600 ESCA system with an Al K α X-ray source (1486.6 eV). The binding energy was calibrated using the C 1s photoelectron peak at 284.6 eV.

Photoelectrochemical (PEC) measurements

The PEC performance of the Si photocathode was evaluated in a three-electrode configuration, with the Si photocathode as the working electrode, Ag/AgCl/sat. KCl as the reference electrode and a platinum foil (2 cm \times 2 cm) as the counter electrode. 1 M HClO₄ (pH 0) aqueous solution was used as the electrolyte. Before PEC tests, the electrolyte was purged with N₂ (Air Liquide) for around 10 minutes to remove dissolved O₂. The potentials obtained from each measurement were converted into values against reversible hydrogen electrode (RHE) using Nernst Equation. An electrochemical workstation (CompactStat. E202050, IVIUM) was used in all PEC measurements. The linear sweep voltammetry (J-V plots), with a scan rate of 50 mV s⁻¹ and chronoamperometry (stability tests) of samples were measured under the irradiation of a 300 W Xenon lamp (Beijing Perfectlight Technology Co Lt, LS-SXE300CUV) equipped with an AM 1.5G filter (100mW cm⁻²). During the 250 h stability test, contamination was observed at the bottom of the porous ceramic plug of the reference electrode, which could be caused by the transfer of electrolyte from the reference electrode^{2,3}.

The applied bias photon-to-current efficiency (ABPE) of above photocathodes was calculated by using the J-V curves with an assumption of 100% Faradic efficiency, according to the following equation:

$$ABPE = \frac{V_{app} \times J_{ph}}{P} \times 100\% \quad (3)$$

where V_{app} is the applied potential (vs. RHE), J_{ph} is the photocurrent density (mA cm⁻²) under AM 1.5G irradiation, and P is the incident illumination intensity (mW cm⁻²) (100 mW cm⁻² in this work).

The IPCE was measured under monochromatic illumination from a 150 W Xe lamp (Zolix LSH-X150) equipped with monochromator (Omni- λ 300) at 0 V vs. RHE using the equation:

$$\text{IPCE}(\%) = \frac{J_{ph} \times 1240}{p \times \lambda} \times 100\% \quad (4)$$

Supplementary Figures:

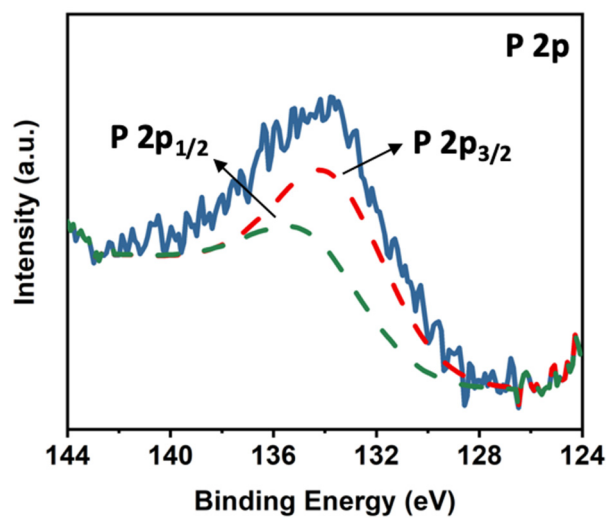


Fig. S1 P 2p XPS spectrum of pn⁺Si sample, which could be deconvoluted into 134.2 eV and 135.3 eV for P₂O₅ and P₄O₁₀⁴⁻, respectively.

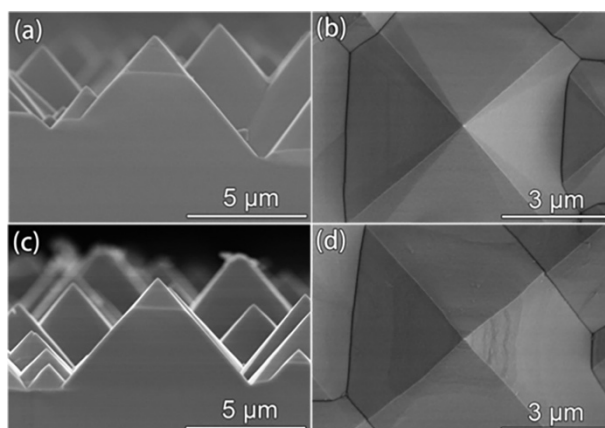


Fig. S2 (a) (b) side and top view SEM images of pristine pyramid Si; (c) (d) side and top view SEM images of pyramid Si after spin coating ADP aqueous solution and annealing.

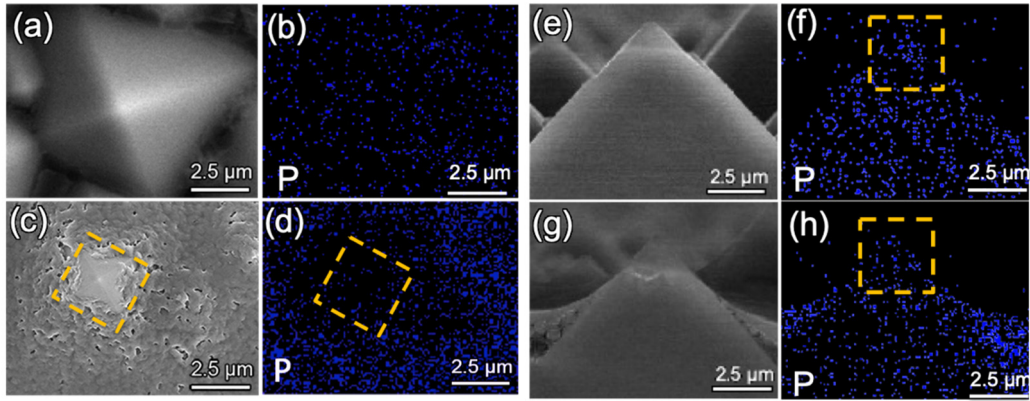


Fig. S3 Top view SEM images and EDX elemental mapping of pyramid Si spin coated with (a, b) ADP aqueous solution, and (c, d) SOD polymer solution; Side view SEM images and EDX elemental mapping of pyramid Si spin coated with (e, f) ADP aqueous solution, and (g, h) SOD polymer solution.

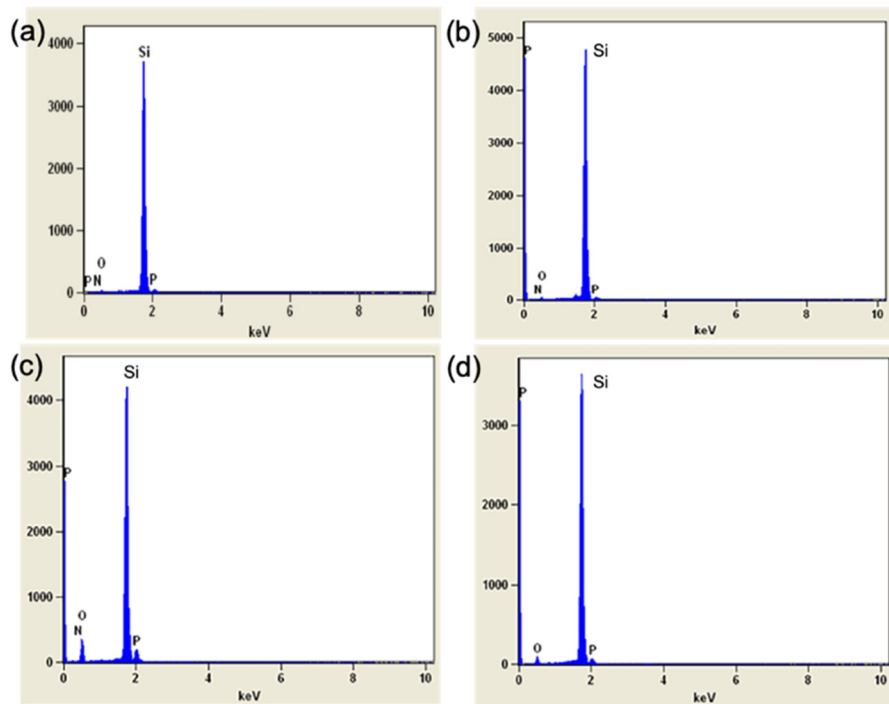


Fig. S4 EDX spectra of (a) top and (b) side view of pyramid Si spin coated by ADP aqueous solution; (c) top and (d) side view of pyramid Si spin coated by SOD polymer solution.

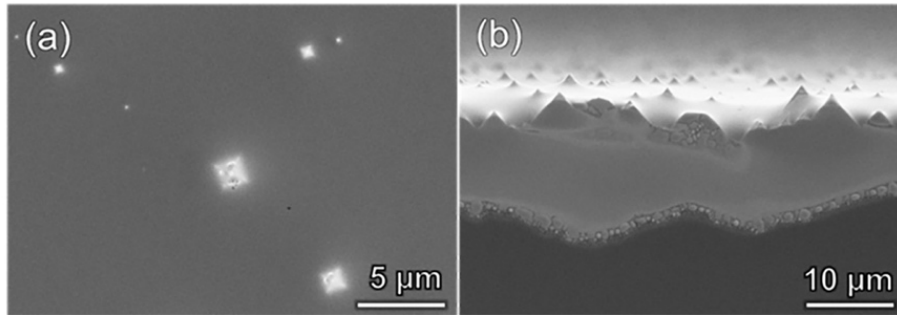


Fig. S5 (a) Top and (b) side view of pyramid p-Si spin coated using 85 wt% H₃PO₄.

Pyramid p-Si substrate spin coated using 85 wt% H₃PO₄, which of much higher viscosity (about 30 times that of ADP aqueous solution) than ADP aqueous solution and SOD polymer solution, was completely covered by a thick layer of dopant.

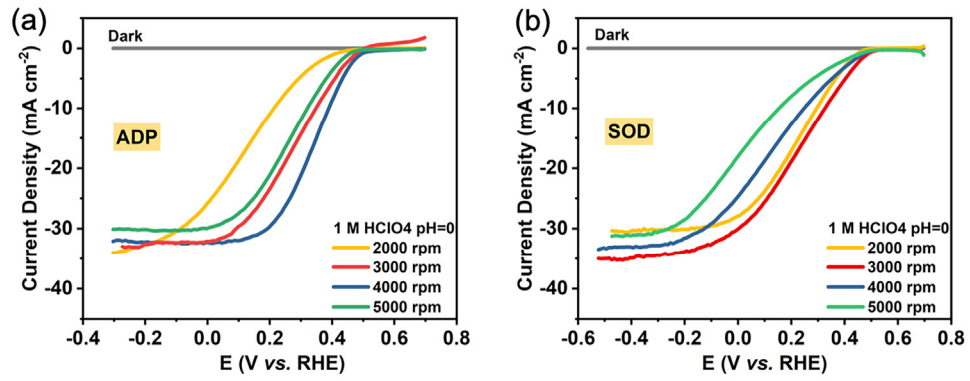


Fig. S6 (a) The optimization of spin speed for pyramid pn⁺Si/Pt photocathodes spin coated with (a) ADP aqueous solution, and (b) SOD polymer solution, measured in 1 M HClO₄ (pH = 0) under AM 1.5G illumination.

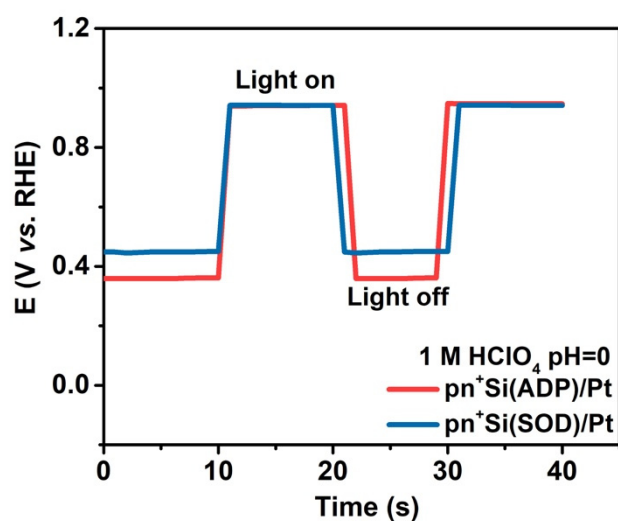


Fig. S7 The open circuit potential versus time of pyramid pn⁺Si(ADP)/Pt and pn⁺Si(SOD)/Pt photocathodes in the dark and under AM 1.5G illumination, in 1 M HClO₄ (pH = 0) electrolyte.

The photovoltage was determined from the difference of open circuit potentials of the sample in the dark and under illumination, respectively⁵. The open circuit potential was measured by monitoring the resting potential of samples (vs. the reference electrode) in the open circuit condition, with the illumination turned on and off manually. The duration of illumination on and off were both 10 s, respectively.

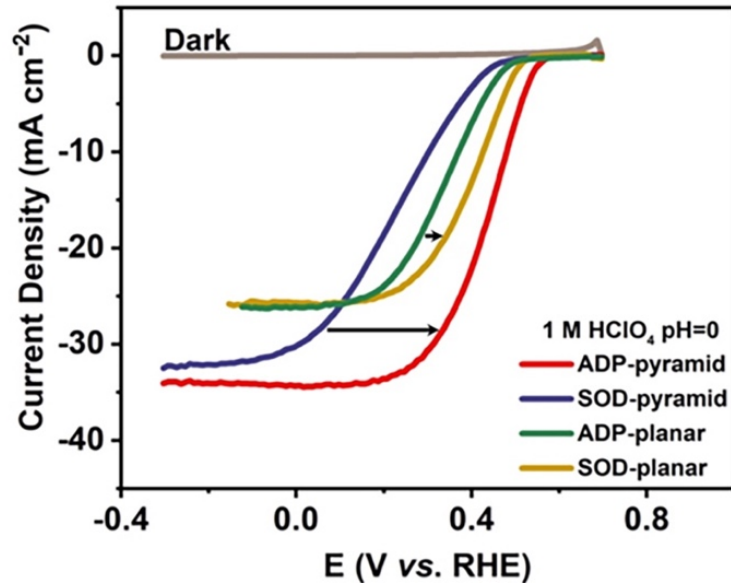


Fig. S8 J-V curves of planar and pyramid pn^+Si/Pt doped by ADP aqueous solution and SOD polymer solution separately. All the measurements are measured in 1 M $HClO_4$ ($pH = 0$) under AM 1.5G illumination.

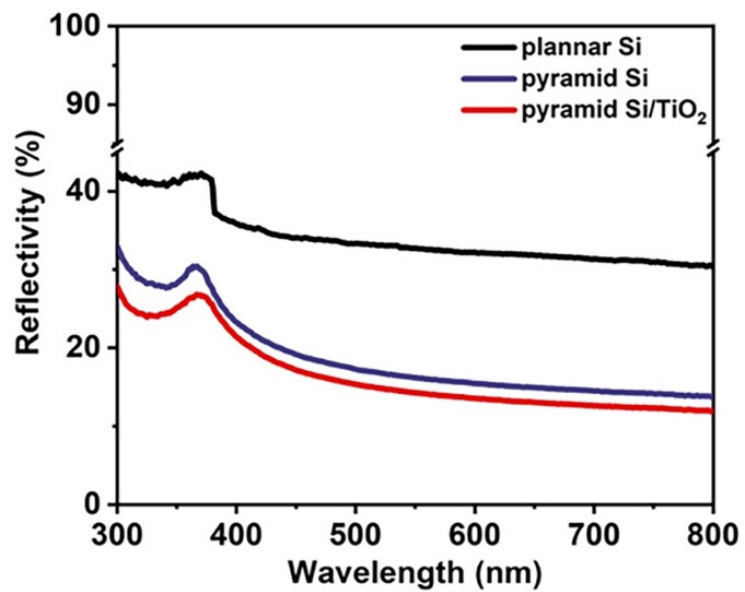


Fig. S9 UV-vis reflection plot of planar and pyramid Si and pyramid Si/TiO₂ photocathodes.

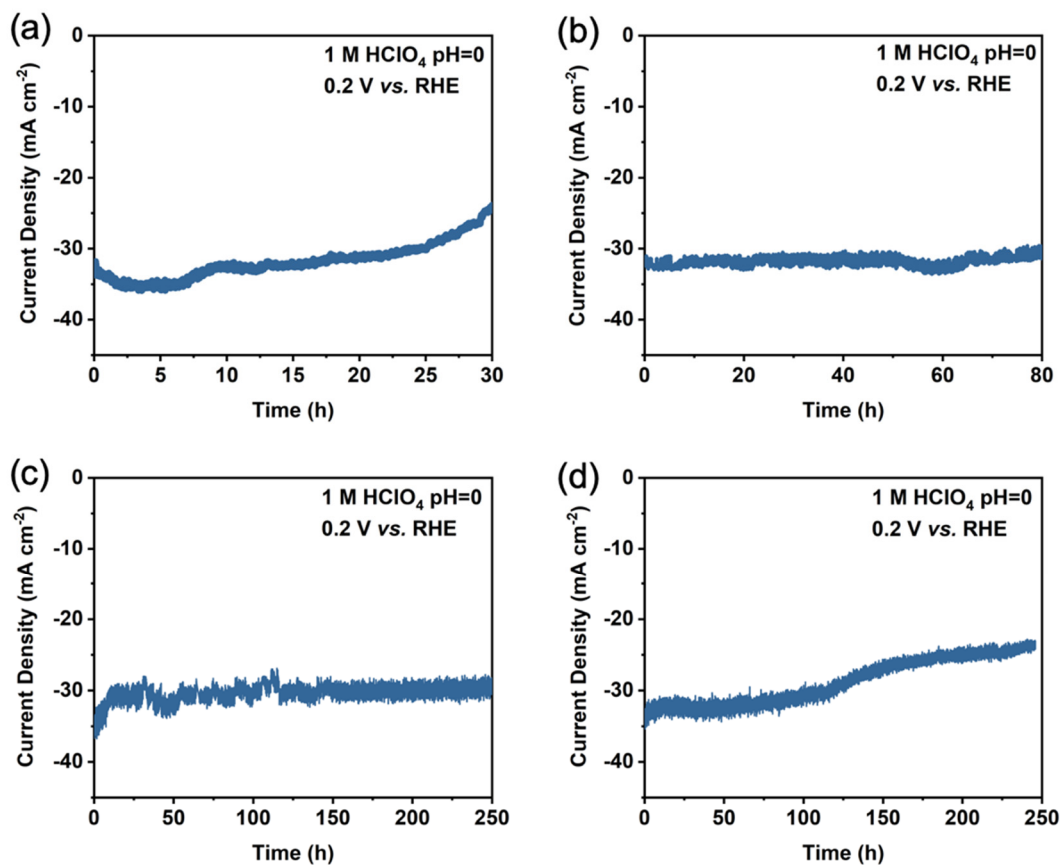


Fig. S10 Stability of four $\text{pn}^+\text{Si(ADP)/TiO}_2\text{/Pt}$ samples from different batches

To thoroughly evaluate the stability of the sample with the batch-to-batch variation considered, four $\text{pn}^+\text{Si(ADP)/TiO}_2\text{/Pt}$ samples from different batches were measured. Two of the samples showed a 250 h stability, while the other two exhibited stabilities of 30 h and 80 h, respectively. The variation of stability might be attributed to the presence of dust particles from the ambient before transferring the sample to the ALD chamber, which results in the formation of pin-holes in TiO_2 protective layer. Therefore, $\text{pn}^+\text{Si(ADP)/TiO}_2\text{/Pt}$ sample is capable of reaching a reproducible stability of 250 h.

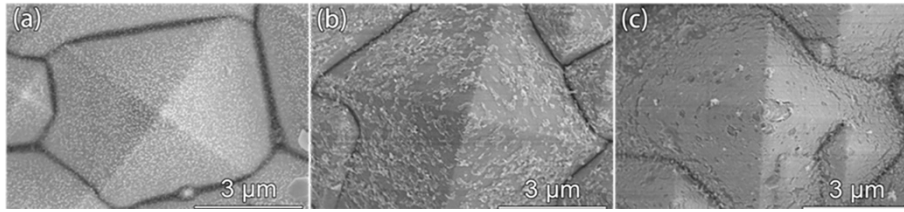


Fig. S11 SEM images of the $\text{pn}^+\text{Si(ADP)/TiO}_2\text{/Pt}$ sample, (a) before stability test, (b) after J-V test and (c) after 250 h long term stability test at 0.2 V vs. RHE in 1 M HClO_4 electrolyte (pH 0) under simulated AM 1.5G illumination.

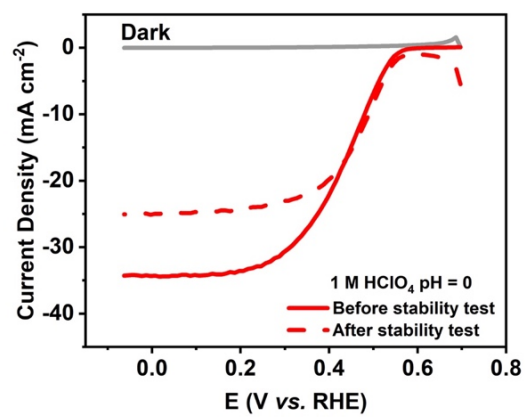


Fig. S12 J-V curves of $\text{pn}^+\text{Si}/\text{TiO}_2/\text{Pt}$ photocathode before and after long term stability test in 1 M HClO_4 ($\text{pH} = 0$) under AM 1.5G illumination.

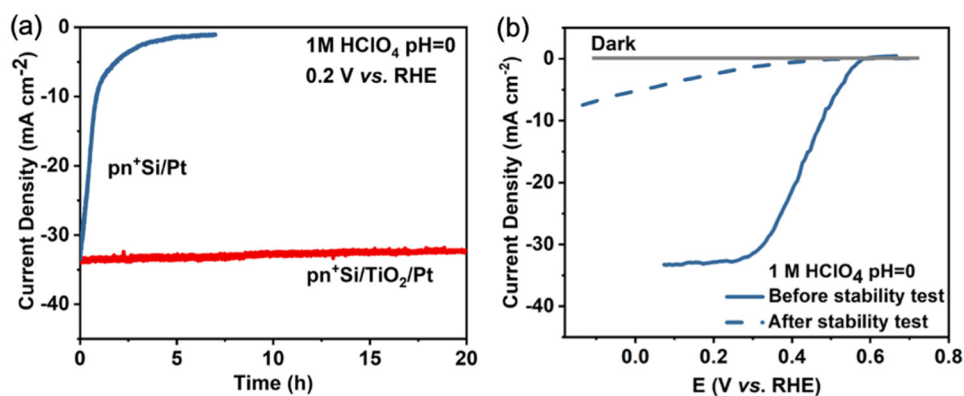


Fig. S13 (a) Stability tests of pn⁺Si/Pt and pn⁺Si/TiO₂/Pt photocathodes at 0.2 V vs. RHE; (b) J-V curves of pn⁺Si/Pt photocathode before and after 7 h stability test. All the measurements are measured in 1 M HClO₄ (pH = 0) under AM 1.5G illumination.

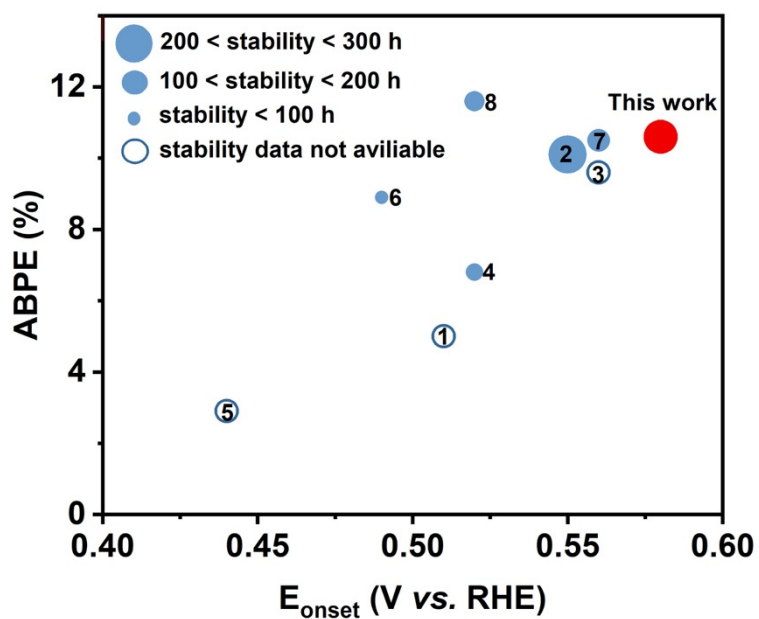


Fig. S14 Performance comparison of pn^+Si photocathodes using different diffusion methods and dopants for PEC HER versus onset potential. (Details in Table S3, with sample numbers representing the symbols in Fig. S14)

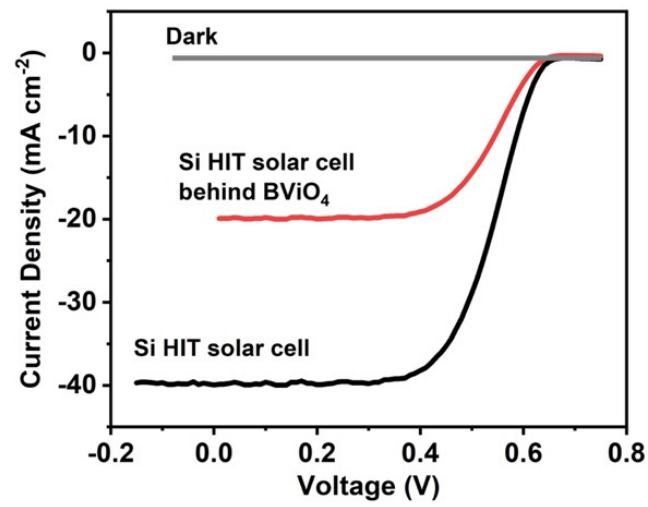


Fig. S15 J-V curves of Si HIT solar cell and Si HIT solar cell behind a BiVO₄ photoanode under AM 1.5G illumination.

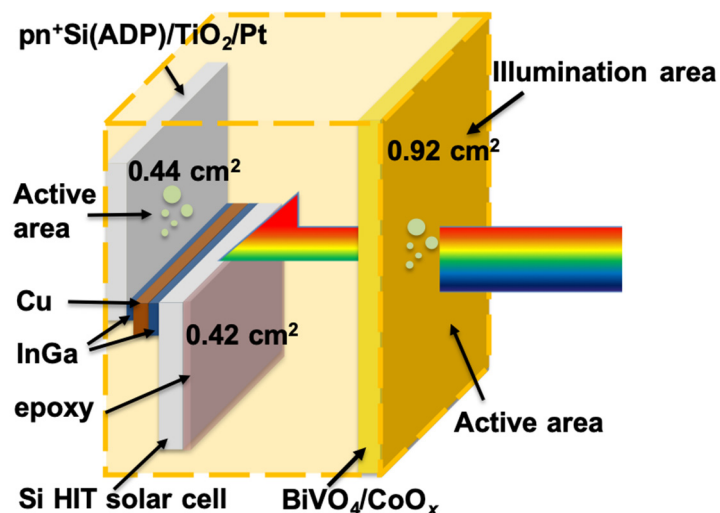


Fig. S16 Schematic illustration of HIT-pn⁺Si(ADP)/TiO₂/Pt photocathode and BiVO₄/CoO_x photoanode tandem cell, with illumination area (yellowish shade) and active area (with bubbles) marked; Si HIT solar cell and pn⁺Si(ADP)/TiO₂/Pt were connected in series using InGa alloy and Cu wire (Si HIT solar cell, Cu and edge of pn⁺Si(ADP)/TiO₂/Pt were encapsulated with epoxy).

For the two-electrode tandem cell (**Fig. 6b** and **d**), the illumination area of the optimized tandem cell was defined by the area of BiVO₄/CoO_x photoanode in direct contact with the electrolyte (0.92 cm²), which is placed in front of the smaller (0.86 cm²) Pt/TiO₂/pn⁺Si(ADP)/InGa/Cu/InGa/HIT photocathode (pn⁺Si(ADP)/TiO₂/Pt is 0.44 cm² and Si HIT is 0.42 cm²). For the three-electrode configuration (**Fig. 6a** and **c**), the illumination area was defined by the photoanode (0.92 cm²) and photocathode (0.86 cm²), respectively, as in normal PEC measurements. The active area of the tandem cell was the area where OER and HER take place (0.92 cm² for photoanode and 0.44 cm² photocathode). All the areas were measured and calibrated by the Image J software.

When calculating current densities for the two-electrode tandem cell (**Fig. 6b** and **d**), the largest illumination cross-section (0.92 cm² of the BiVO₄/CoO_x photoanode) was used as the denominator. For the three-electrode configuration (**Fig. 6a** and **c**), the illumination area (0.92 cm² for photoanode and 0.86 cm² photocathode), rather than the active area, was used as the denominator. The STH efficiency was calculated based on these photocurrent densities.

Supplementary Tables:

Table. S1 Viscosity of tested samples.

Sample	Time/s					Average	Viscosity /cP
	1	2	3	4	5		
1 H ₂ O	77.56	77.74	77.98	78.22	78.16	77.93	0.8937
2 ADP aqueous solution	84.67	85.06	85.07	85.72	85.59	85.22	1.0262
3 SOD polymer solution	158.90	161.08	161.78	161.56	162.63	161.69	1.5790

The viscosity (η) of above samples was calculated according to the following equation:

$$\eta_2 = \eta_1 \frac{\rho_2 t_2}{\rho_1 t_1}$$

where ρ is the density (g cm^{-3}), t is the time (s) obtained. Ubbelohde viscometer was used in this test at the temperature of 25 °C.

($\rho_1 = 0.997 \text{ g cm}^{-3}$, $\rho_2 = 1.047 \text{ g cm}^{-3}$, $\rho_3 = 0.849 \text{ g cm}^{-3}$)

Range of η_{SOD} given by our supplier is 1.45-1.82 cP (dopants with various concentration of alcohol) at 25 °C.

Table. S2 Counts of P peaks in EDX spectrums.

Sample	P counts	Full-scale counts	Atomic concentration/%
ADP (top view)	96	3718	2.58
ADP (side view)	83	4789	1.73
SOD (top view)	367	4213	8.71
SOD (side view)	177	3644	4.86

Table. S3 Performance comparison of pn⁺Si photocathodes using different diffusion methods and dopants for PEC HER.

#	Year	Phosphorous source	Morphology	Photoelectrode structure	E(onset) (V vs. RHE)	ABPE (%)	Stability (h)	Electrolyte	Ref
This work	2019	ADP aqueous solution	pyramid	pn ⁺ Si/TiO ₂ /Pt	0.58	10.6	250	1 M HClO ₄	
1	2015	SOD polymer solution	microwire	pn ⁺ Si/Pt	0.51	5	-	0.5 M H ₂ SO ₄	6
2	2018	SOD polymer solution	microwire	pn ⁺ Si/NiSi/NiMo	0.55	10.1	288	1 M KOH	7
3	2011	CeP ₅ O ₁₄	planar	pn ⁺ Si/Pt	0.56	9.6	-	0.5 M H ₂ SO ₄	8
4	2015	PClO ₃	pyramid	pn ⁺ Si/Al ₂ O ₃ /Pt	0.52	6.8	100	0.5 M K ₂ SO ₄ +0.5 M H ₂ SO ₄	9
5	2015	PClO ₃	microwire	pn ⁺ Si/Pt	0.44	2.9	-	0.5 M H ₂ SO ₄	10
6	2016	PClO ₃	pyramid	pn ⁺ Si/Pt@SiO ₂	0.49	8.9	22	0.5 M K ₂ SO ₄ +0.5 M H ₂ SO ₄	11
7	2017	PClO ₃	pyramid	pn ⁺ Si/Pt ₂ /TiO ₂	0.56	10.5	168	1 M HClO ₄	12

Supplementary References:

1. X. Chang, T. Wang, P. Zhang, J. Zhang, A. Li and J. Gong, *J. Am. Chem. Soc.*, 2015, **137**, 8356-8359.
2. M. P. Mousavi and P. Buhlmann, *Anal. Chem.*, 2013, **85**, 8895-8901.
3. A. Yakushenko, D. Mayer, J. Buitenhuis, A. Offenhausser and B. Wolfrum, *Lab Chip*, 2014, **14**, 602-607.
4. A. Thøgersen, M. Syre, B. Retterstol laisen and S. Diplas, *J. Appl. Phys.*, 2013, **113**, 044307.
5. L. Ji, M. D. McDaniel, S. Wang, A. B. Posadas, X. Li, H. Huang, J. C. Lee, A. A. Demkov, A. J. Bard, J. G. Ekerdt and E. T. Yu, *Nat. Nanotechnol.*, 2014, **10**, 84-90.
6. M. R. Shaner, J. R. McKone, H. B. Gray and N. S. Lewis, *Energy Environ. Sci.*, 2015, **8**, 2977-2984.
7. W. Vijselaar, R. M. Tiggelaar, H. Gardeniers and J. Huskens, *ACS Energy Lett.*, 2018, 1086-1092.
8. S. W. Boettcher, E. L. Warren, M. C. Putnam, E. A. Santori, D. Turner-Evans, M. D. Kelzenberg, M. G. Walter, J. R. McKone, B. S. Brunschwig, H. A. Atwater and N. S. Lewis, *J. Am. Chem. Soc.*, 2011, **133**, 1216-1219.
9. R. Fan, W. Dong, L. Fang, F. Zheng, X. Su, S. Zou, J. Huang, X. Wang and M. Shen, *Appl. Phys. Lett.*, 2015, **106**.
10. C. W. Roske, E. J. Popczun, B. Seger, C. G. Read, T. Pedersen, O. Hansen, P. C. K. Vesborg, B. S. Brunschwig, R. E. Schaak, I. Chorkendorff, H. B. Gray and N. S. Lewis, *J. Phys. Chem. Lett.*, 2015, **6**, 1679-1683.
11. R. Fan, C. Tang, Y. Xin, X. Su, X. Wang and M. Shen, *Appl. Phys. Lett.*, 2016, **109**, 233901.
12. R. Fan, W. Dong, L. Fang, F. Zheng and M. Shen, *J. Mater. Chem. A*, 2017, **5**, 18744-18751.